MICROSTRUCTURE OF AIR PLASMA-SPRAYED NiAl COATING

KAROL IŽDINSKÝ[1]*, JURAJ DUFEK[1], JOZEF IVAN[1], MILINA ZEMÁNKOVÁ[1], PAVOL MINÁR[1], ZITA IŽDINSKÁ[2]

The microstructure of NiAl coating formed by air plasma spraying of ball milled NiAl30 powder is studied in this paper. Numerous chemical and structural inhomogeneities were determined by light microscopy, microhardness measurements, SEM, TEM, and EDX analysis. The coating is formed by a mixture of phases including α-Al and γ-Ni based solid solutions, β-NiAl, martensitic NiAl, and γ'-Ni_3Al intermetallic compounds. Amorphous, partially crystallized and crystallized fine grained Al_2O_3 oxides with spinel structure were also determined.

K e y w o r d s: NiAl coating, air plasma spraying, microstructure, TEM studies, intermetallic phases

MIKROŠTRUKTÚRA POVLAKU NiAl ZHOTOVENÉHO PLAZMOVÝM STRIEKANÍM NA VZDUCHU

V práci sú uvedené výsledky štúdia mikroštruktúry povlaku NiAl zhotoveného plazmovým striekaním na vzduchu prášku NiAl30, ktorý bol pripravený mletím v guľovom mlyne. Pozorovania svetelnou mikroskopiou, elektrónovou riadkovacou a transmisnou mikroskopiou, merania mikrotvrdosti a analýzy vykonané energiovo-disperznou spektroskopiou ukázali, že povlak obsahuje početné štruktúrne nehomogenity, ako aj nehomogenity chemického zloženia. Povlak sa skladá zo zmesi fáz na báze tuhých roztokov α-Al a γ-Ni, z intermetalických zlúčenín β-NiAl, martenzitu NiAl a γ'-Ni_3Al. V mikroštruktúre sa zistila prítomnosť amorfných, čiastočne skryštalizovaných a jemnozrnných kryštalických Al_2O_3 oxidov so štruktúrou spinelového typu.

1. Introduction

Due to its quite unique physical and mechanical properties, e.g. low density, high melting point, good oxidation resistance, and metal-like electrical and thermal

[1] Ústav materiálov a mechaniky strojov SAV, Račianska 75, 831 02 Bratislava 3, Slovak Republic
[2] Katedra materiálov a technológií STU, Pionierska 15, 812 31 Bratislava 1, Slovak Republic
* corresponding author, e-mail: ummsizd@savba.sk

conductivity, the intermetallic NiAl compound can be found in a large variety of engineering applications ranging from electronic components to hot sections of gas turbine engines for aircraft propulsion systems [1–3].

The Ni-Al alloy coatings benefiting by exothermic reactions between Ni and Al during plasma spraying [4] have gained quite exceptional position in the philosophy and application of thermal barrier coatings (TBC). These are typically applied to gas turbine engine blades and vanes in order to reduce their operating temperatures and thus increasing the component durability. A typical duplex TBC system is formed by thermally insulating ceramic top coating applied over an oxidation--resistant metallic bond coating. The most common top coating is air plasma-sprayed yttria stabilized zirconia possessing good strain tolerance and low thermal conductivity. Bond coatings typically consist of NiAl, NiCrAl or MCrAlY alloys providing a good thermal expansion match between the top coat and substrate and inhibiting the oxidation of the substrate due to formation of protective Al_2O_3; NiO; CoO and Cr_2O_3 oxide layers [5].

Ni-Al coatings are mostly produced by air plasma spraying or low pressure plasma spraying of composite powders where Ni core is cladded by Al envelope. As these particles are melted, mutual exothermic reaction between Ni and Al in intimate contact takes place, what results in a better adherence of coating to the substrate.

We have shown in our previous work [6] that the intimate contact between Al and Ni can be achieved also by ball milling of elemental Al and Ni powders. The microstructural studies performed on NiAl30 powders confirmed that substantial part of powder particles exhibit fine lamellar microstructure resulting from severe deformation, fracture and welding in the ball milling process. Lamellar domains are formed by elemental Ni and Al as well as by ordered β-NiAl. Nanocrystalline Ni_2Al_3 was locally recognized, too. No amorphous phase was observed in the studied microstructure.

NiAl30 ball milled powder was consecutively used to produce air plasma-sprayed coating. This article presents the results of microstructural studies performed with this as-sprayed coating.

2. Experimental material and procedure

NiAl30 ball milled nickel base binary powder containing 30 mass % of aluminium with sizes below 45 μm was plasma sprayed onto a steel substrate at a total power input of 32 kW. Argon with a gasflow rate of 5 l/min was used as a plasma carrying gas and hydrogen and argon with gasflow rates of 12 l/min and 40 l/min, respectively, were used as plasma forming gases. As-sprayed coating with the average thickness of 0.25 mm was removed from the substrate and subjected to the microstructural analysis.

Light microscopy (LM) and Vickers microhardness measurements, scanning electron microscopy (SEM), transmission electron microscopy (TEM) and energy--dispersive X-ray spectroscopy (EDX) were used for the structural studies. Samples for LM and SEM studies were prepared by conventional metallographic techniques. The thin foil preparation for TEM observations was accomplished by ion milling.

SEM observations were performed using the JEOL 5310 electron microscope operated at the accelerating voltage of 15 kV, TEM observations were carried out at a JEOL JEM 100 C analytical electron microscope operated at 100 kV. The analyses including bright field and dark field image observations with selected area electron diffraction (SAED) were employed. EDX analyses were performed using a Kevex Delta class IV spectrometer with an ultra-thin window detector (Kevex Quantum detector). Ion milling was performed using the BAL-TEC RES 010 rapid etching system.

3. Results

Typical structures of air plasma sprayed NiAl coating in the longitudinal and cross sectional views are shown in Fig. 1. It clearly appears that the structure is formed by heterogeneous mixture of phases. Bright matrix and darkly appearing inclusions and pores can be distinguished even at low magnifications. The hetero-

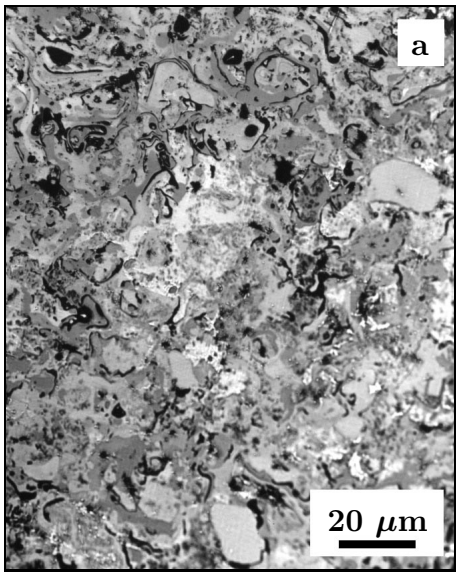

Fig. 1a. Light micrograph of the longitudinal section of NiAl coating.

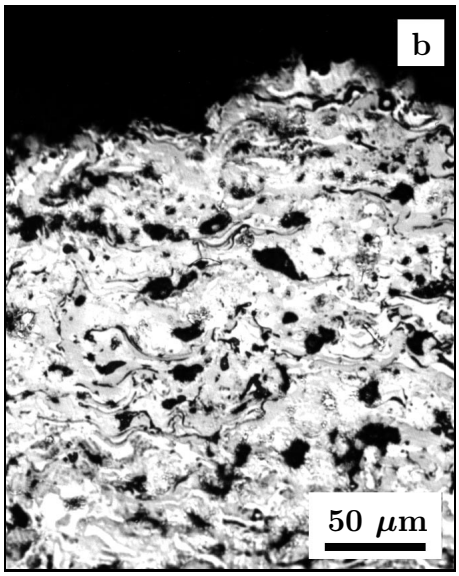

Fig. 1b. Light micrograph of the cross section of NiAl coating.

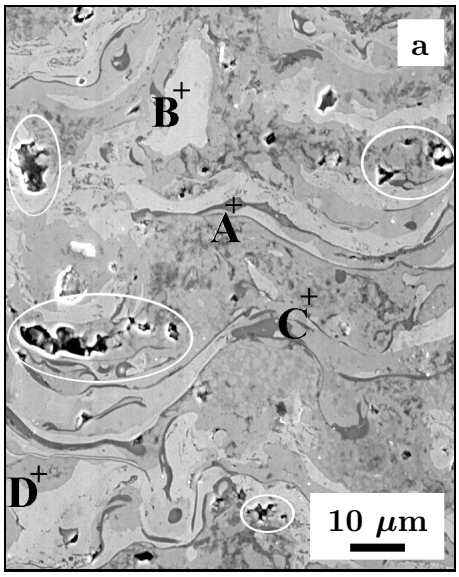

Fig. 2a. Microstructure in the cross-section of the NiAl coating (SEM).

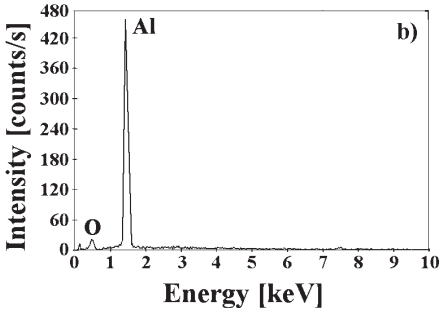

Fig. 2b. EDX spectrum acquired by point analysis at A (energy-dispersive X-ray spectroscopy).

geneity is underlined by the fact that no etching had to be applied to reveal the overall structure of the coating.

Vickers microhardness measurements showed that the hardness of the coating gives wide scattered values ranging from 88 to 290 HV 0.01. The average hardness determined from 30 measurements in the cross section of the coating was 130 HV 0.01 with standard deviation of 72 HV 0.01.

Microstructure of the coating as revealed by the SEM is shown in Fig. 2a. Here mostly lamellar matrix with thin elongated inclusions in the lamellae boundary regions dominate the microstructure. Further, localized areas with relatively higher densities of open pores can be also observed. Typical locations are white encircled in Fig. 2a. EDX analysis confirmed that the darkly appearing elongated inclusions contain predominantly Al and O, sometimes also with little amounts of Ni. Therefore, they can be identified as oxide stringers often met in the air plasma sprayed coatings [7]. Typical spectrum acquired by point analysis in an oxide inclusion is shown in Fig. 2b.

The matrix itself is formed by a mixture of phases differing by shades of grey. These phases contain different amounts of Al and Ni. Generally it appears, that as far as chemical composition is concerned, the bright areas contain mostly Ni

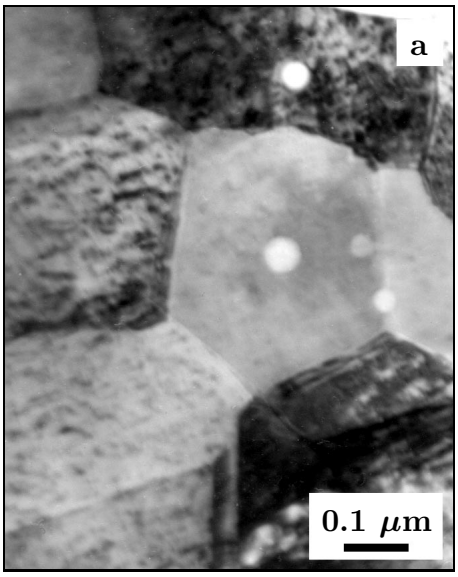

Fig. 3a. γ-Ni grains in the microstructure of the NiAl coating (TEM, BF image).

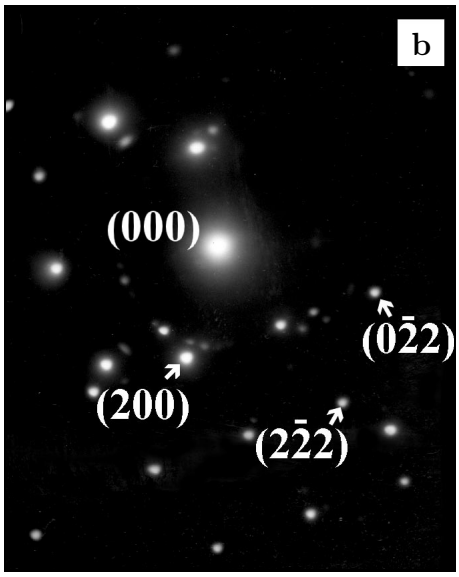

Fig. 3b. SAED pattern corresponding to $[0\bar{1}\bar{1}]$ zone of of γ-Ni.

T a b l e 1. Quantitative EDX point analysis in the coating shown in Fig. 2a

Element	Position of point analysis		
	B	C	D
Al [mass %]	3.1	42.5	82.8
Ni [mass %]	96.9	57.5	17.2

and the darkest regions are dominated by Al. Regions displaying middle levels of grey contain both Al and Ni in significant amounts. Typical results of quantitative EDX analysis are presented in Table 1.

TEM studies confirmed that areas with very high contents of Ni refer to face-centered cubic nickel based solid solution γ-Ni. Typical fine-grained microstructure of these regions is shown in Fig. 3. White globular particles in the γ-Ni grains refer to amorphous oxide inclusions. Corresponding SAED pattern confirms that no superlattice reflections indicating the presence of γ'-Ni_3Al appear in this location.

Regions with high concentration of Al were identified by TEM as face-centered cubic Al based solid solution α-Al. They do not reveal so fine-grained microstructure as γ-Ni. Typical example with dislocation systems is shown in Fig. 4.

Areas where both elemental constituents, i.e. Al and Ni appear in significant

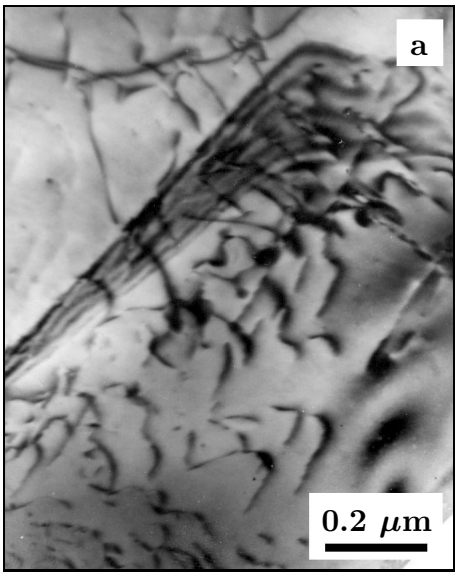

Fig. 4a. Dislocations in the Al region of NiAl coating (TEM, BF image).

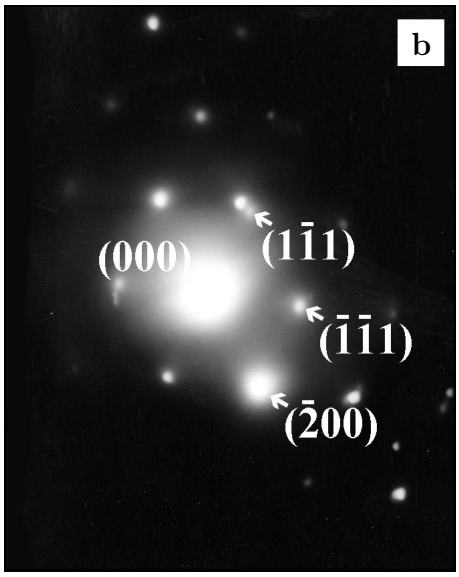

Fig. 4b. SAED pattern corresponding to [011] zone of Al.

amounts, are formed by intermetallic phases or contain these phases dispersed in the matrix metal. Most frequently appearing is the body centered cubic of the CsCl type (B2) based solid solution β-NiAl. Typical example is shown in Fig. 5. Also the martensitic NiAl with face-centered tetragonal Ll_0 structure with typical twinned morphology appears quite often. Finally face-centered cubic of the Cu_3Au (Ll_2) type γ'-Ni_3Al precipitates can be found in the γ-Ni matrix. All three intermetallic compounds are shown in Fig. 6. Typical twinned morphology of martensitic NiAl is further shown in Fig. 7. White globular particle in Fig. 7a refers again to amorphous oxide inclusions that were often met in the coating microstructure.

Finally, oxide stringers were analyzed by TEM. It appeared that amorphous, partially crystallized and fully crystallized oxides were to be found in the coating. The structure of the crystallized oxides was identified as face-centered cubic structure of γ-Al_2O_3. A typical example is shown in Fig. 8. Partially crystallized and amorphous oxides are shown in Figs. 9 and 10.

4. Discussion of results

Plasma-sprayed coatings are mostly formed by disc-shaped microstructural units, often referred to as "splats" [8–10]. These obtain their geometry as a result of the impingement of the molten particle onto the substrate surface. Splashing

Fig. 5a. β-NiAl in the microstructure of NiAl coating (TEM, BF image).

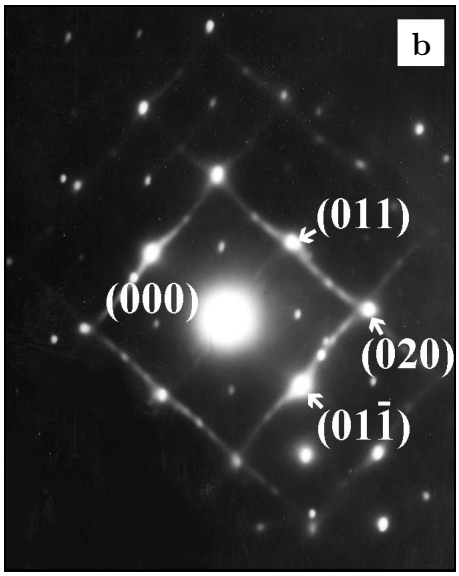

Fig. 5b. SAED pattern corresponding to [100] zone of β-NiAl.

is known to occur not by flowing on the surface but by jetting away from the impinged droplet center to the periphery [11]. Further unmelted or poorly melted particles can be incorporated in the coating. These and the splashing phenomenon of spreading particles often play a significant role in the formation of pores or generally termed, "improperly flattened zones" [7]. Finally, reaction products of the scale-forming elements with the dissociated oxygen atoms entrapped into the plasma jet from the environment, form oxide inclusions usually identified due to their elongated shapes as oxide stringers in predominantly air plasma-sprayed coatings [7].

Powered by the energy input of the plasma jet, powder particles undergo a series of metallurgical, chemical and phase transformations in the deposition process. These are significantly affected by the size, composition and microstructure of initial powders as well as by the parameters of the plasma spraying and can be traced by the structural analysis of the as-sprayed coating.

As revealed by the light microscopy, SEM and corresponding EDX analysis, all the typical structural components including "splats", unmelted or poorly melted particles, pores, "improperly flattened zones", oxide stringers and inclusions can be easily recognized in the structure of the NiAl coating. It indicates that the as-sprayed coating represents a mixture of various phases resulting from the chemical,

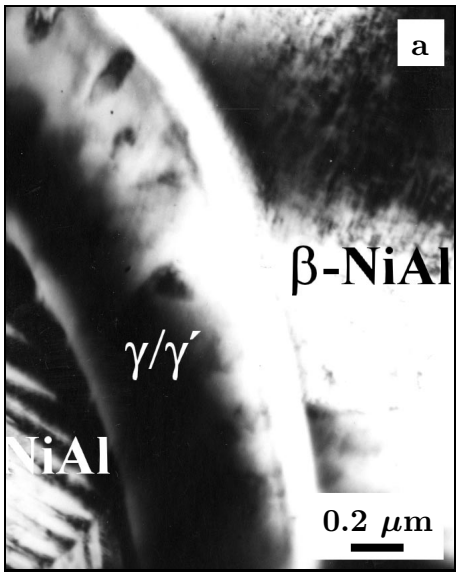

Fig. 6a. Neighbouring phases of martensitic NiAl, γ/γ' and β-NiAl in the microstructure of NiAl coating (TEM, BF image).

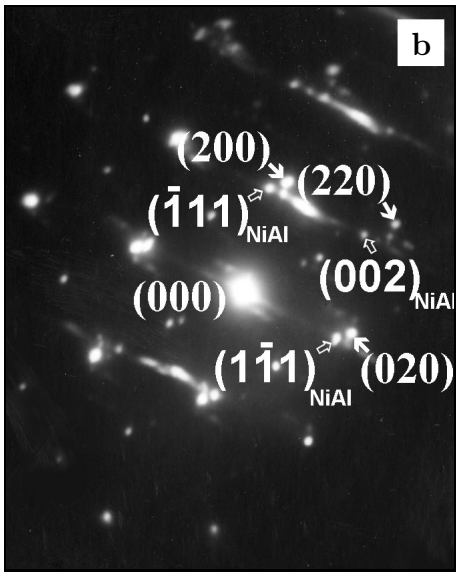

Fig. 6b. SAED patterns corresponding to $[\bar{1}\bar{1}0]$ zone of martensitic NiAl superimposed on $[00\bar{1}]$ zone of γ/γ'.

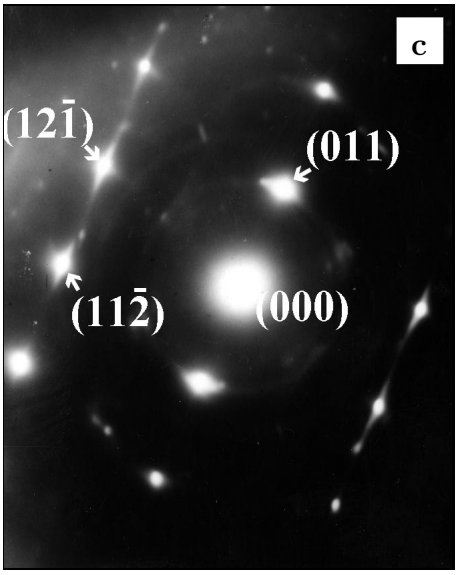

Fig. 6c. SAED pattern corresponding to $[\bar{3}1\bar{1}]$ zone of β-NiAl.

mechanical and thermal treatment accompanying the spraying process. The variety of phases is underlined not only by the EDX analysis, confirming various portions of Al and Ni constituents in different locations of the coating, but also by the results of microhardness measurements giving wide scattered values ranging from 88 to 290 HV 0.01. The lower values are suspected to be influenced by the presence of hidden pores and other structural inhomogeneities close to the measured region.

As Al and Ni form various intermetallic compounds differing only by few atomic %, their identification is certainly not quite reliable by means of EDX. Therefore the TEM analysis pro-

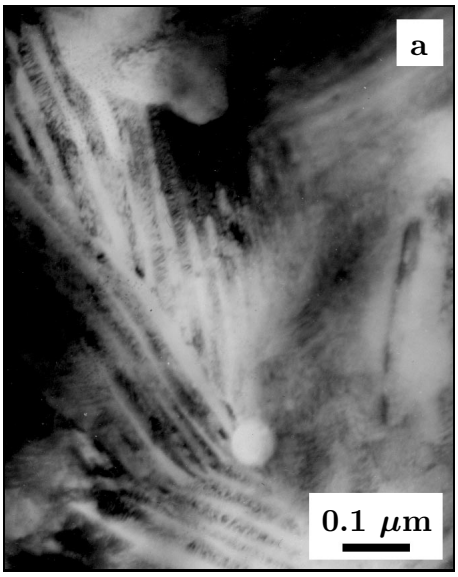

Fig. 7a. Martensitic NiAl in the microstructure of NiAl coating (TEM, BF image).

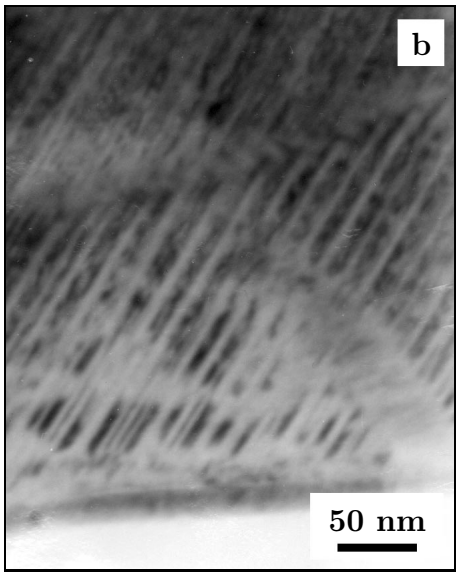

Fig. 7b. Martensitic NiAl in the microstructure of NiAl coating (TEM, BF image).

vided clear evidence of present phases and their morphology. It was confirmed that Al and Ni based solid solutions that had been primarily identified in the initial powder particles did appear also in the as-sprayed coating. It means that the mixing of elemental constituents in the ball milling process followed by air plasma spraying were not sufficient to form equilibrium phases regarding the overall chemical powder composition. The deposition process was apparently too short and the temperature too low to promote sufficient diffusion for setting the thermodynamic balance in some locations. However, the thermodynamic balance can be expected after deliberately introduced subsequent thermal treatment of the coating.

Formation of all expected intermetallic phases including β-NiAl, martensitic NiAl and γ'-Ni_3Al was confirmed in zones where Al and Ni elemental constituents were in intimate contact, and the energy input was high enough to promote sufficient diffusion for the required phase transformations. In the Ni-Al phase diagram, the B2 phase is stable over a wide composition region of 32–58 at.% Al at elevated temperatures and approximately 41–55 at.% Al at room temperature [12]. Martensitic transformation requires Al content less than $\sim$ 37 at.% [13, 14], material exposure to elevated temperatures ($>\sim$ 1000 °C) and sufficiently fast cooling rates to suppress the β-γ' transformation [15]. Respecting the current chemical het-

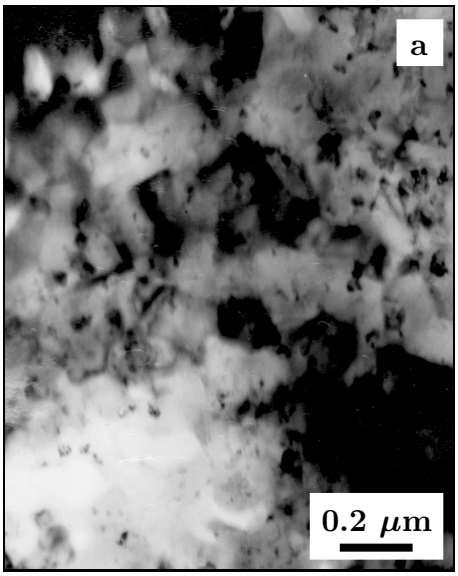

Fig. 8a. Fine grained γ-Al_2O_3 oxide in the microstructure of NiAl coating (TEM, BF image).

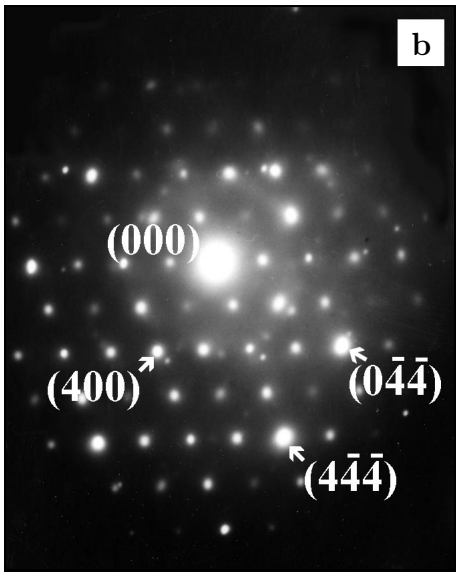

Fig. 8b. SAED pattern corresponding to $[01\bar{1}]$ zone of γ-Al_2O_3.

erogeneity and not very well defined thermal history of individual plasma sprayed powders, it can be easily assumed that all three preconditions are frequently met in numerous events giving rise to martensitic transformation of the β-NiAl phase. γ'-Ni_3Al is an equilibrium decomposition product of γ-Ni and β-NiAl in the Ni-Al binary system. Its presence indicates that for some locations the cooling was not so rapid to fully suppress the running diffusion. The direct formation of γ'-Ni_3Al cannot be excluded, too. This is in agreement with thermodynamic calculations giving evidence that the Ni-Al reactions forming intermetallic compounds are all exothermic. As reported, the heat released by the formation of NiAl at the temperature of 1600 K is 139.63 $kJ \cdot mol^{-1}$ and 176.05 $kJ \cdot mol^{-1}$ by Ni_3Al [4].

As the initial microstructure of ball milled powder was already heterogeneous and far from equilibrium, the formation of numerous phases with various morphologies in the process of plasma spraying is not surprising. Thermal, kinetic and chemical factors mostly govern the process of new phase formation. As these parameters are not constant but undergo permanent change from powder to powder, formation of different phases on micrometric scale takes place. Subsequent thermal treatment is expected to stimulate further phase transformations directed towards the thermodynamic equilibrium of the coating.

No oxides were observed in the initial powder. It means that all the oxide

Fig. 9. Partially crystallized oxide inclusion in the microstructure of NiAl coating (TEM, BF image).

Fig. 10. Amorphous oxide inclusion in the microstructure of NiAl coating (TEM, BF image).

inclusions revealed in the coating had to be formed during the air-plasma spraying due to the mutual reaction of Al with oxygen. The presence of amorphous, partially crystallized and fine grained fully crystallized Al_2O_3 oxides was confirmed in the current coating. The appearance of amorphous oxides is not surprising at all, as it had been revealed already in paper [16] dealing with the microstructure of air plasma-sprayed NiCrAlY coating. However, exclusively amorphous oxides were determined in the as-sprayed NiCrAlY coating. Amorphous to crystalline transformation took place gradually in the subsequent thermal treatment of the coating performed at 850 ℃ [17, 18]. The appearance of crystallized γ-Al_2O_3 oxides in the current NiAl coating can be explained in terms of less dramatic temperature decrease after the impingement of the molten particle onto the substrate, when compared with the NiCrAlY coating. This can be also due to the exothermic character of reactions accompanying the NiAl compound formation in the deposition process.

γ-Al_2O_3 oxide belongs to the metastable Al_2O_3 phases with the structure of defect spinels. It should be stressed, that no possible indexing scheme allowed for the existence of thermodynamically stable rhombohedral α-Al_2O_3. This is however in good agreement with the results [19–21], confirming that the initial formation

of metastable Al_2O_3 phases seems to be a general phenomenon of alumina forming alloys.

5. Conclusions

The microstructure of NiAl coating formed by air plasma spraying of ball milled NiAl30 powder was studied in this paper.

Numerous chemical and structural inhomogeneities were determined.

The coating is formed by a mixture of phases including α-Al and γ-Ni based solid solutions, β-NiAl, martensitic NiAl and γ'-Ni_3Al intermetallic compounds.

Amorphous, partially crystallized and crystallized fine-grained Al_2O_3 oxides with spinel structure were also determined.

Acknowledgements

The authors gratefully acknowledge Mr. P. Petrík and Mr. S. Chovanec for the preparation of plasma sprayed samples.

REFERENCES

[1] MURTY, B. S.—RANGANATHAN, B. S.: Int. Mat. Rev., *43*, 1998, p. 101.
[2] LAPIN, J.: Kovove Mater., *40*, 2002, p. 209.
[3] LAPIN, J.—PELACHOVÁ, T.—BAJANA, O.: Intermetallics, *8*, 2000, p. 1417.
[4] CHEN, H. C.—PFENDER, E.: Thin Solid Films, *280*, 1996, p. 188.
[5] ÇELIK, E.—AVCI, E.—YILMAZ, F.: Surf. Coat. Tech., *97*, 1997, p. 361.
[6] IŽDINSKÝ, K.—IŽDINSKÁ, Z.—DUFEK, J.—IVAN, J.—ZEMÁNKOVÁ, M.: Kovove Mater., *41*, 2003, p. 106.
[7] CHOI, H.—YOON, B.—KIM, H.—LEE, Ch.: Surf. Coat. Tech., *150*, 2002, p. 297.
[8] ALCALÁ, J.—GAUDETTE, F.—SURESH, S.—SAMPATH, S.: Mater. Sci. Eng., *A 316*, 2001, p. 1.
[9] OHMORI, A.—LI, C. J.: Thin Solid Films, *201*, 1991, p. 241.
[10] SAMPATH, S.—HERMAN, H.: J. Thermal Spray Tech., *5*, 1996, p. 445.
[11] MOREAU, C.—GOUGEON, P.—LAMONTAGNE, J.: J. Therm. Spray Technol., *4*, 1995, p. 25.
[12] HANSEN, M.—ANDERKO, K.: Constitution of Binary Alloys. New York 1958.
[13] KUMAR, K. S.—MANNAN, S. K.—VISWANADHAM, R. K.: Acta Mater., *40*, 1992, p. 1201.
[14] MURTHY, A. S.—GOO, E.: Acta Mater., *41*, 1993, p. 3435.
[15] ZHANG, Y.—HAYNES, J. A.—PINT, B. A.—WRIGHT, I. G.—LEE, W. Y.: Surf. Coat. Tech., *163–164*, 2003, p. 19.
[16] IŽDINSKÝ, K.—IVAN, J.—ZEMÁNKOVÁ, M.—KOLENČIAK, V.: Kovove Mater., *36*, 1998, p. 367.
[17] IŽDINSKÝ, K.—IVAN, J.—ZEMÁNKOVÁ, M.: Kovove Mater., *38*, 2000, p. 329.
[18] IŽDINSKÝ, K.—IVAN, J.—ZEMÁNKOVÁ, M.: Kovove Mater., *39*, 2001, p. 316.
[19] DOYCHAK, J.—SMIALEK, J. L.—MITCHELL, T. E.: Metall. Trans., *20 A*, 1989, p. 499.
[20] SCHUMANN, E.—RÜHLE, M.: Acta Metall. Mater., *42*, 1994, p. 1481.
[21] SMIALEK, J. L.—GIBALA, R.: Metall. Trans., *14A*, 1983, p. 2143.

Received: 29.4.2003